Structure Determination based on Continuous Diffraction from Macromolecular Crystals

Henry N. Chapman [1,2,3] ***and Petra Fromme*** [4,5]

[1] Center for Free-Electron Laser Science, DESY, 22607 Hamburg, Germany.

[2] Department of Physics, University of Hamburg, 22761 Hamburg, Germany.

[3] Center for Ultrafast Imaging, University of Hamburg, 22761 Hamburg, Germany.

[4] School of Molecular Sciences, Arizona State University, Tempe, Arizona 85287-1604, USA.

[5] Biodesign Center for Applied Structural Discovery, Arizona State University, Tempe, Arizona 85287, USA.

To whom correspondence should be addressed: henry.chapman@desy.de and pfromme@asu.edu

Keywords: continuous diffraction, diffuse scattering, X-ray crystallography, X-ray Free-Electron Lasers, Photosystem II

Published in Current Opinion in Structural Biology, doi:10.1016/j.sbi.2017.07.008

Abstract

Bright and coherent X-ray sources, such as free-electron lasers, have spurred the development of new methods for determining the structures of biological macromolecules. In particular, single-molecule diffraction is highly desired, as it would abolish the need for crystallization. Further, it provides considerably more diffraction intensity information than is needed to solve a structure. This is unlike crystal diffraction where the diffraction intensity information is usually insufficient for direct phasing. To overcome the challenge of weak scattering signals from single molecules, direct phasing approaches in coherent diffractive imaging have been combined with micro-crystals in several imaginative ways. One of these, using micro-crystals with translational disorder, has been used to phase continuous femtosecond X-ray diffraction data from Photosystem II complexes, offering a paradigm shift in crystallography.

Introduction

X-ray crystallography has long been the "work horse" for structure determination of biomolecules, with over 80% of the more than 100,000 structures in the protein data bank solved by this method. There are no restrictions on the size of the (bio) molecule that can be solved by X-ray structure determination; they have ranged from single amino acids to large molecular assemblies like ribosomes and viruses.

An important limitation for the method of X-ray crystallography is that molecules must be ordered in a three-dimensional crystal lattice. The growth of large well-ordered single crystals is a major bottleneck for X-ray structure analysis of difficult to crystallize proteins like membrane proteins, large complexes and molecules with flexible regions. Furthermore, packing of molecules into a crystalline lattice can alter the structure and function of the molecule. However, there are examples where proteins have been crystallized in their fully functional form and where native-like activity was measured in the crystal. One such example is Photosystem II, where the crystalline complex has been shown to be fully functional in water splitting and in oxygen evolution when illuminated by light [1],[2]. By contrast, tight packing of molecules in a highly ordered crystal can restrict motion, and can induce unnatural conformations and alter functional activity [3].

The strength of the diffraction signal depends on the product of the crystal volume and the incident X-ray exposure. Large crystals are required, not because we do not have X-ray beams that are intense enough, such as are available at microfocus synchrotron beamlines, but because exposure is limited by X-ray damage of the crystal under investigation. X-rays cause photoionization and a cascade of electron ionizations that lead to complex radiolysis processes including photo-reduction (which is especially severe for biomolecules containing metals), bond cleavage, and destruction of the crystal and its constituent biomolecules. The exposure is limited by the tolerable dose of the crystal which is about 30 MGy under cryogenic conditions [4].

With the advent of X-ray free-electron lasers (XFEL) [5], the major challenges of conventional X-ray crystallography were solved. XFELs are the most powerful X-ray sources that have ever been built. They have a peak brightness that exceeds that of beams produced at 3rd generation synchrotron radiation facilities by nine orders of magnitude.

When focused to a small spot, an XFEL pulse turns any solid material into a plasma, at pulse fluences above about 10^8 photons/μm^2. With femtosecond-long pulses, FEL X-rays are diffracted before significant radiation-induced structural changes occur [6],[7]. Thus, by 'outpacing' radiation damage the need to grow large single crystals no longer exists. At the timescale of femtoseconds, atoms are effectively frozen, so there is also no need to cryogenically cool the sample and measurements can be carried out at room temperature. However, only a single snapshot diffraction pattern can be recorded from an object under these conditions, Thus, the method, referred to as serial femtosecond crystallography (SFX), requires passing crystals rapidly across the beam to record diffraction patterns one at a time [8-10] each from a fresh crystal, ideally at the repetition rate of the XFEL. SFX data sets usually consist of tens of thousands of X-ray diffraction snapshots from small (1-5 μm range), randomly oriented single crystals which are indexed and combined to provide accurate structure factors for structure determination. For most SFX structures, phases have been determined by molecular replacement. Only recently have examples of experimental phasing been published [11-13].

Single Particle Diffraction

The availability of bright XFEL pulses provided an opportunity for determining structures of single non-periodic particles [14],[15] by building up diffraction data from individual macromolecules, as is done with crystals in serial crystallography [6]. The motivation for working with single particles is twofold. Firstly, there is no need to crystallize the sample. Secondly, the continuous diffraction obtained in the absence of periodicity can be easily phased *de novo*, due to the availability of high redundancy diffraction data [16]. Such an approach however comes with the disadvantage that, even with the power of an XFEL, total diffraction from a single molecule is exceedingly weak. This makes the method extremely challenging. Nevertheless, single molecule diffraction is highly desired since the increase in the information content of diffraction from a single object, as compared to diffraction from a crystal of that object, is enough to solve the phase problem. When diffraction is not limited only to measurements at Bragg peaks there are generally more independent measurements (or "samples") of the diffraction

intensities from a non-periodic object than needed to describe the object to the resolution determined by the highest scattering angles to which that diffraction is observed [17]. The surplus of measured information content over that required to describe the object can be a factor of four or more, depending on the shape of the object [18]. This factor does not depend on resolution, which means that atomic resolution is not required. This is in stark contrast to diffraction from a crystal, where intensities are only sampled at the Bragg positions. These generally only give half the information needed to describe the object and to solve its structure.

Diffraction from a non-periodic object does not consist of Bragg peaks which arise due to translational symmetry. Rather, it takes the form of a continuously varying intensity as "speckles" of a width that is inversely proportional to the object's size. This is analogous, to the speckle pattern observed by shining an optical laser onto a uniformly rough surface, such as a painted wall. The continuous diffraction can be phased using any of a class of algorithms that iteratively constrain the solution to be consistent with both the measured diffraction intensities and any prior knowledge about the object's structure [16]. This additional information need not be detailed, and may simply be that the object fits within a certain box that is smaller than the extent of its autocorrelation function [19] or that the electron density is positive. Such algorithms originate from early work in electron microscopy by Gerchberg and Saxton [20], and were first demonstrated in the X-ray regime by Miao and colleagues [21]. The development of the shrink-wrap algorithm [22] made it possible to dynamically update the constraints on the object's shape and size during iteration, allowing the first "diffraction before destruction" imaging at the soft X-ray free-electron laser in Hamburg (FLASH) [23]. A comprehensive experimental investigation into high-resolution 3D X-ray imaging of a non-periodic structure based on coherent diffraction provides a close analogy to crystallographic phasing, albeit where half a billion phases were retrieved and without any requirement for atomic resolution [24]*.

The development of single particle imaging of molecules and virus particles has had to contend with the fact that without the large amplification of signal due to the crystal lattice, the diffraction from such objects is very weak. While this can be addressed by using very intense X-ray pulses, such pulses also give rise to a significant extraneous

background in the diffraction pattern, which has required considerable effort to reduce [25]*. To emerge from this was the goal of making the best of both worlds. Specifically, to combine continuous diffraction having a high information content with a large signal-to-background ratio made possible by collecting data on a multitude of identical particles.

Between Single Molecules and Crystals

One early idea as to how to increase the signal-to-background ratio of the diffraction from identical but non-periodic objects was to align them (for example, using a polarized laser) as they streamed past a steady X-ray or electron beam [26]. In this way, the collected diffraction signal would accumulate over time. Although the degree of alignment of a molecule depends on its polarizability, which could limit the resolution that can be achieved [27], the feasibility of such an approach was demonstrated using pulsed-laser alignment of small molecules in the gas phase [28].

As crystallographers know, objects can be aligned by placing them in contact with one another, as in a crystal. An early study considered using membranes containing integral proteins. The membranes could be layered one atop the other thereby fixing at least one orientation (the direction normal to the membrane) [29]. Depending on the degree of order this stacking approach would give rise to a single column of Bragg peaks in the ordered direction, or a continuous rod of diffraction intensity. In the latter case, the Fourier transform of the intensity rod gives the entire autocorrelation of the thickness profile of the membrane. Stroud and Agard came up with the idea of phasing this iteratively by constraining to zero the electron density above and below the membrane [29], a so-called “compact support” constraint. However, later work showed that a given 1D diffraction pattern can arise from many different density profiles; that is, a unique 1D density profile cannot be found [30], [31]. Subsequently, Spence *et al* [32] demonstrated that the membrane compact support constraint could be successfully applied to 2D crystals where the diffraction is not just limited to one continuous rod of diffraction intensity but consists of a lattice of rods.

Renewed interest in diffraction intensity rods emerged during the first XFEL diffraction experiments of protein nanocrystals when it was noted that lattice truncation at crystal

boundaries gives rise to measurable signals between Bragg peaks [8]. Each lattice point of the crystal is convolved with the Fourier transform of the shape of the crystal, giving access to finer "samples" of the underlying molecular transform. Spence *et al* [33] proposed a method to extract that transform from serial diffraction data of nanocrystals. Since each crystal in such a measurement can have a different size and shape, each diffraction snapshot will consist of different shape transforms around each Bragg peak. However, the underlying molecular transform should always be the same. By summing all patterns in 3D reciprocal space one obtains the result of a common molecular transform multiplied by Bragg peaks with the incoherently averaged shape transform. This average 3D shape can be ascertained simply by taking the average of all Wigner-Seitz cells (where each cell is defined as the volume encompassing points that are closest to a given reciprocal lattice point than any other lattice point), which can then be divided from the data in the neighborhood of each Bragg peak. This method was successfully demonstrated with artificial crystals [34]*. It lead to the realization that the continuous diffraction obtained this way crucially depends on the molecular arrangement at the surface of the crystal [35],[36].

At the other end of the single particle-to-crystal size spectrum, the idea of iterative phasing has been applied directly to Bragg diffraction data from macroscopic crystals. Indeed, density modification uses a simple iterative algorithm to successively apply constraints in reciprocal space (matching the measured diffraction intensities) and real space (flattening the solvent). More recently, the charge-flipping algorithm [37] and Feinup's hybrid input-output algorithm [38]* have been applied to crystal data. These algorithms work provided there is an excess of diffraction information recorded over that needed to describe the electron density, such as happens when the crystal has a high solvent fraction [39]*.

The tantalizing question remained, Is there an intermediate regime between crystallography and single particle imaging that offers the best of both worlds?

Diffraction from Imperfect Crystals

The defining property of a crystal is translational symmetry. This correlation over long length scales (long-range order) results in the constructive interference of waves diffracted from each molecule into sharp Bragg peaks. The width of the Bragg peak is inversely related to the range of order. Real crystals, and macromolecular crystals in particular, exhibit many kinds of faults and irregularities. The degree of order in the presence of these types of effects can often be described by a correlation function that may be anisotropic in both position in the crystal and in the direction of correlation relative to the crystal lattice. The form of this correlation can often be ascertained from diffraction effects that appear as broadened or modulated Bragg peaks, streaks of diffuse diffraction, and speckles [40].

Speckle or continuous diffraction is not uncommon. It has been referred to in the literature also as "diffuse scattering". Early detectors such as film and charge-coupled devices (CCDs) posed challenges to the measurement of weak speckle diffraction. However, pioneering experiments investigated its potential for revealing conformational heterogeneity and protein dynamics [41-43];[44] and for assisting in structure refinement [45]. Continuous diffraction was noted to follow the point group symmetry of the crystal [42]. Some frustration was expressed that understanding intramolecular displacements is made difficult because continuous diffraction is dominated by rigid-body translations of whole molecules [46.]. In a recent study [47]*, certain features of the diffraction could be correlated (at around 50% correlation) with various models of disorder, such as "translation, libration, screw", liquid-like motions, and normal modes. However, this continuous diffraction was not considered for use in facilitating the determination of molecular structure.

Continuous diffraction from imperfect crystals has been studied for decades. These investigations failed to recognize that the inherent signal, which is indeed dominated by rigid-body motion of whole molecules, is of much greater value for the determination of the structure than it is in characterizing the displacements themselves. The discovery that led to this paradigm shift was the demonstration that crystals of the large membrane protein complex, Photosystem II [1], feature very small translational disorder of rigid-body units that are the entire Photosystem II complex [48] **.

The effect of random translations of rigid molecular units from the ideal periodic crystal lattice is illustrated in Fig. 1. A shift of a molecule by a vector $\vec{\sigma}$ from its position in the lattice modulates the diffracted wavefield from that molecule by a phase ramp $\exp(-2\pi i\vec{\sigma}\cdot\vec{q})$. Here, the magnitude of the wave-vector transfer $\vec{q}$ is equal to $2\sin\theta/\lambda$ for a scattering angle 2θ and wavelength λ. In the extreme case of a gas of aligned molecules shown in Fig. 1a, the random displacements have no correlation length and the corresponding phases will be completely random and uncorrelated to each other. For a large number of molecules (*N*), these uncorrelated phases give rise to an incoherent sum of the diffraction of each object. This will have a strength *N* times that of the diffraction of a single object. The uncorrelated phases prevent the conditions of constructive interference that give rise to Bragg peaks.

Consider instead only small displacements $\vec{\sigma}$ of whole molecules from their ideal lattice positions. At a Bragg peak corresponding to a particular resolution length $d = 1/q$, the wavefield of the displaced molecule will combine with those of others with a phase error of $2\pi\sigma/d$ if that displacement is in the direction corresponding to the Bragg peak. For example, a displacement of 1.5 Å would cause destructive interference (a phase shift of π) at a Bragg peak corresponding to 3 Å resolution. Small random displacements of all molecules in the crystal with a mean square displacement of $<\sigma^2>$ will lead to random phases for scattering angles at high enough resolution, giving an incoherent sum of the "single molecule" diffraction in a similar fashion to the gas of aligned molecules, but only at the higher resolution as shown in Fig. 1b. At low resolutions ($d >> \sigma$), the phase errors from the displacements will be small, which allows the constructive interference of Bragg peaks with little or no continuous diffraction. In general, the Bragg intensities are modulated by the well-known Debye-Waller factor, $\exp(-4\pi^2\sigma^2q^2)$, of the same form as the so-called "temperature factor" that arises from atomic displacements, whereas the continuous diffraction increases contrariwise with q as $1-\exp(-4\pi^2\sigma^2q^2)$.

There are two important implications of translational disorder in a crystal. One is that the continuous diffraction of a translationally-disordered crystal may extend to resolutions far beyond Bragg peaks. Accordingly, the resolution of useful information for structure determination is not necessarily limited by the extent (resolution) of the Bragg peaks. The

second is that the continuous diffraction may be phased, as discussed above, without the need for a structural model. In the recent demonstration on microcrystals of Photosystem II [48]**, Bragg peaks were observed to a resolution of about 4.5 Å (Fig. 2), consistent with a σ value of 2 Å [49]. In contrast, continuous diffraction was observed to a resolution of 3.5 Å and was limited only by the size of the detector and the number of diffraction patterns recorded. The continuous diffraction was phased using the difference map algorithm [50], extending the resolution of the Bragg reflections by 1 Å to 3.5 Å [48]**.

It must be stressed that the Bragg diffraction and continuous diffraction report on different underlying structures, and so far phasing has been accomplished by considering these separately [42]. The Bragg peaks arise from the periodic structure of the crystal and, if given their true phases, the structure factors would generate, through a Fourier synthesis, the contents of the unit cell. In Photosystem II this consists of a particular arrangement of four dimers. The diffraction of this arrangement of objects lead to interferences, which of course encode their relative positions, similar to the diffraction from a pair of identical pinholes which consists of fringes that modulate the concentric-ring "Airy pattern" fringes of a single hole. The continuous diffraction, on the other hand, is the incoherent sum of the diffraction of the different rigid units (the four orientations of dimers in the case of Photosystem II). There are no interfering fringes that relate these units since they are independent. The concern that high-resolution Bragg data may somehow explain the success of phasing the continuous diffraction [51] is thus illogical; it can only supply incorrect information to the phasing algorithm. A further development of the technique will be to combine both sets of data into one iterative algorithm.

The origin of the continuous diffraction as the incoherent sum of the molecular diffraction from Photosystem II dimers was confirmed by several tests: i) The autocorrelation map computed directly from the continuous intensities was of finite extent with a boundary of the correct size and shape as Photosystem II molecules. ii) The distribution of the intensities in the continuous diffraction followed Wilson statistics. iii) The diffraction could be phased iteratively, producing a 3D image with much clearer

definition of structural elements such as α helices, even though the phasing algorithm had no knowledge of such structures. Indeed, the real-space support constraint used in the iterative phasing process, at 8.9 Å resolution, included no indication of these structures. iv) Using an improved analysis [49], the continuous diffraction computed from the atomic model fitted to the electron density image agreed with the measured diffraction data with a correlation coefficient of better than 0.75 (Fig. 3).

Continuous diffraction requires careful measurement protocols as compared to Bragg peak measurements. The latter can be delineated easily from unstructured background, as arises from air scatter, the physical crystal support and mother liquor. Continuous diffraction from a disordered crystal contains as many diffracted photons as are present in the Bragg peaks at the same resolution from an ordered crystal. However, the photons are spread out over many more pixels than Bragg peaks, making the signal (per pixel) much weaker. For an average spacing of 10 pixels between Bragg peaks, for example, the continuous diffraction signal per pixel will be 1% of that of the Bragg peaks from a perfectly ordered crystal.

Conclusions

It is interesting to ask whether structure determination using continuous diffraction generated from translational disorder requires XFEL pulses. Continuous diffraction had been observed in many systems measured at synchrotron sources since the 1980's, although it was only the community interested in conformational dynamics that had taken the necessary care to characterize it [52],[47]*. The method of serial crystallography using XFEL pulses provided ideal conditions to measure the weak continuous diffraction with very low background, and the snapshot diffraction patterns could readily be assembled in 3D reciprocal space without suffering from blurring of the continuous diffraction that would occur while rotating the crystal during the exposure [53].

The method of using continuous diffraction for structure determination may also have benefited from the use of small crystals for SFX. As is well appreciated in nanoscience, a small crystal is less likely to have growth defects caused by convection, sedimentation and vibration and high mosaicity than its macroscopic counterpart. This size issue is

important because the evaluation of continuous diffraction data relies on minute random translational displacements. In a large crystal with multiple mosaic blocks, the variation in the orientation of blocks may lead to a blurring of the continuous diffraction. Nanocrystals may still feature intrinsic disorder, as is induced by weak crystal contacts and/or thermal motions within the crystals. These might become more prominent as crystal size decreases, because a larger fraction of molecules are located at the crystal surface where they have fewer contacts with adjoining molecules and thereby may feature enhanced positional flexibility. This has been observed in electron microscopic images of nanocrystals [54]*.

It remains to be seen how many macromolecular crystal systems exhibit translational disorder. However, it is reasonable to speculate that many do, given that the stiffness of macromolecules is much greater than that of the crystals they form such that the weakest structural connections are at the crystal contacts. This does not preclude rotational disorder of rigid molecules in these crystals, which must be accounted for when phasing the data to produce an image of the electron density. There might be a reason why the first case of phasing continuous diffraction from crystals was from a large membrane protein complex. Membrane proteins derive naturally from a membrane and are crystallized either in the form of protein-detergent micelles or protein-lipid complexes. In these types of crystals translational disorder might be more pronounced than rotational disorder. Rotational disorder might expose hydrophobic regions of the membrane protein to the aqueous environment as the protein would rotate out of plane in relation to the 2D lipid or detergent "layer" network in the crystals. In-plane rotation may in some cases be constrained by contacts with neighboring molecules in the membrane. Examples of strong continuous diffraction from membrane protein crystals have been observed previously (see, for example, ref [55]) and for many, structures have not yet been determined. These are now prime targets for imaging based on continuous diffraction.

Acknowledgements

This work was funded by the European Research Council under the European Union's Seventh Framework Programme ERC Synergy Grant 609920 "Frontiers in Attosecond X-

ray Science: Imaging and Spectroscopy (AXSIS)". H.N.C. additionally acknowledges project funds to DESY CFEL by the Helmholtz Association. P.F. acknowledges funding by the BioXFEL Science Technology Center (award 1231306); and the US National Institutes of Health (NIH), National Institute of General Medical Sciences grant R01 GM095583.

Figure Captions

Fig. 1: Diffraction from an ensemble of identical objects in the same orientation depends on their correlations. (a) A gas of aligned objects gives rise to the incoherent sum of their continuous diffraction. (b) A crystal with translational disorder consists of Bragg peaks formed from the constructive interference of diffraction from all objects, at resolutions lower than the disorder length divided by 2π. The incoherent sum of single-object diffraction dominates at higher resolutions. (c) Perfect crystals produce only the coherent sum of diffraction from the periodic array of scatterers.

Fig. 2: Weak continuous diffraction (a) was observed in individual snapshot diffraction patterns recorded from Photosystem II crystals at the LCLS [48]. When 2,885 patterns were merged in a common frame of reference (defined by the indexed lattice) in 3D reciprocal space, the signal-to-noise ratio of the continuous diffraction markedly improved, and extended significantly beyond the Bragg peaks (b). The continuous diffraction could be phased using an iterative phasing algorithm to obtain a 3D image of the electron density of the Photosystem II dimer. A detail shows the improvement obtained from performing a structural refinement using the Bragg data only (to a resolution of 4.5 Å) (c) as compared with the combined use of the Bragg and continuous diffraction (to a resolution of 3.5 Å) (d).

Fig. 3: (a) Central slices of the merged volume of experimental continuous diffraction intensities, normal to the (010) lattice vector, compared with (b) the same section of the simulated continuous diffraction assuming a rotational disorder of 1° root mean square (RMS) and a translational disorder of 2 Å RMS. (c) The difference of the experimental and simulated intensities, shown on the same color scale as (a) and (b). (d) Plot of the Pearson correlation coefficient in resolution shells between the experimental and simulated data, further confirming that rigid-body displacements of the Photosystem II dimer account for the observed continuous diffraction.

References

1. Kupitz C, Basu S, Grotjohann I, Fromme R, Zatsepin NA, Rendek KN, Hunter MS, Shoeman RL, White TA, Wang DJ, et al.: **Serial time-resolved crystallography of photosystem II using a femtosecond X-ray laser**. *Nature* 2014, **513**:261-+.
2. Zouni A, Jordan R, Schlodder E, Fromme P, Witt HT: **First Photosystem II crystals capable of water oxidation**. *Biochimica Et Biophysica Acta-Bioenergetics* 2000, **1457**:103-105.
3. Corbett MS, Mark AE, Poger D: **Do All X-ray Structures of Protein-Ligand Complexes Represent Functional States? EPOR, a Case Study**. *Biophys J* 2017, **112**:595-604.
4. Owen RL, Rudino-Pinera E, Garman EF: **Experimental determination of the radiation dose limit for cryocooled protein crystals**. *Proceedings of the National Academy of Sciences of the United States of America* 2006, **103**:4912-4917.
5. Emma P, Akre R, Arthur J, Bionta R, Bostedt C, Bozek J, Brachmann A, Bucksbaum P, Coffee R, Decker FJ, et al.: **First lasing and operation of an \aa ngstrom-wavelength free-electron laser**. *Nat Photon* 2010, **4**:641--647.
6. Neutze R, Wouts R, van der Spoel D, Weckert E, Hajdu J: **Potential for biomolecular imaging with femtosecond X-ray pulses**. *Nature* 2000, **406**:752-757.
7. Barty A, Caleman C, Aquila A, Timneanu N, Lomb L, White TA, Andreasson J, Arnlund D, Bajt S, Barends TRM, et al.: **Self-terminating diffraction gates femtosecond X-ray nanocrystallography measurements**. *Nature Photonics* 2012, **6**:35-40.
8. Chapman HN, Fromme P, Barty A, White TA, Kirian RA, Aquila A, Hunter MS, Schulz J, DePonte DP, Weierstall U, et al.: **Femtosecond X-ray protein nanocrystallography**. *Nature* 2011, **470**:73-77.
9. Schlichting I: **Serial femtosecond crystallography: the first five years**. *Iucrj* 2015, **2**:246-255.
10. Chavas LMG, Gumprecht L, Chapman HN: **Possibilities for serial femtosecond crystallography sample delivery at future light sourcesa)**. *Structural Dynamics* 2015, **2**:041709.
11. Barends TRM, Foucar L, Botha S, Doak RB, Shoeman RL, Nass K, Koglin JE, Williams GJ, Boutet S, Messerschmidt M, et al.: **De novo protein crystal structure determination from X-ray free-electron laser data**. *Nature* 2014, **505**:244--247.
12. Nass K, Meinhart A, Barends TRM, Foucar L, Gorel A, Aquila A, Botha S, Doak RB, Koglin J, Liang MN, et al.: **Protein structure determination by single-wavelength anomalous diffraction phasing of X-ray free-electron laser data**. *Iucrj* 2016, **3**:180-191.
13. Batyuk A, Galli L, Ishchenko A, Han GW, Gati C, Popov PA, Lee MY, Stauch B, White TA, Barty A, et al.: **Native phasing of x-ray free-electron laser data for a G protein-coupled receptor**. *Sci Adv* 2016, **2**:e1600292.

14. Seibert MM, Ekeberg T, Maia FR, Svenda M, Andreasson J, Jonsson O, Odic D, Iwan B, Rocker A, Westphal D, et al.: **Single mimivirus particles intercepted and imaged with an X-ray laser**. *Nature* 2011, **470**:78-81.
15. Hantke MF, Hasse D, Ekeberg T, John K, Svenda M, Loh D, Martin AV, Timneanu N, Larsson DS, van der Schot G, et al.: **A data set from flash X-ray imaging of carboxysomes**. *Sci Data* 2016, **3**:160061.
16. Chapman HN, Nugent KA: **Coherent lensless X-ray imaging**. *Nat Photon* 2010, **4**:833--839.
17. Sayre D: **Some implications of a theorem due to Shannon**. *Acta Crystallographica* 1952, **5**:843.
18. Elser V, Millane RP: **Reconstruction of an object from its symmetry-averaged diffraction pattern**. *Acta Crystallographica Section A* 2008, **64**:273-279.
19. Fienup JR: **Phase retrieval algorithms: a comparison**. *Applied Optics* 1982, **21**:2758-2769.
20. Gerchberg RW, Saxton O: **Practical algorithm for determination of phase from image and diffraction plane pictures**. *Optik* 1972, **35**:237-246.
21. Miao J, Charalambous P, Kirz J, Sayre D: **Extending the methodology of X-ray crystallography to allow imaging of micrometre-sized non-crystalline specimens**. *Nature* 1999, **400**:342-344.
22. Marchesini S, He H, Chapman HN, Hau-Riege SP, Noy A, Howells MR, Weierstall U, Spence JCH: **X-ray image reconstruction from a diffraction pattern alone**. *Physical Review B* 2003, **68**:140101.
23. Chapman HN, Barty A, Bogan MJ, Boutet S, Frank M, Hau-Riege SP, Marchesini S, Woods BW, Bajt S, Benner WH, et al.: **Femtosecond diffractive imaging with a soft-X-ray free-electron laser**. *Nat Phys* 2006, **2**:839--843.
* 24. Chapman HN, Barty A, Marchesini S, Noy A, Hau-Riege SP, Cui C, Howells MR, Rosen R, He H, Spence JC, et al.: **High-resolution ab initio three-dimensional x-ray diffraction microscopy**. *J Opt Soc Am A Opt Image Sci Vis* 2006, **23**:1179-1200.

** The first demonstration of phasing a 3D volume of continuous diffraction from a non-periodic object*

* 25. Aquila A, Barty A, Bostedt C, Boutet S, Carini G, dePonte D, Drell P, Doniach S, Downing KH, Earnest T, et al.: **The linac coherent light source single particle imaging road map**. *Structural Dynamics* 2015, **2**.

** This paper describes the collaborative project , led by the LCLS, of more than 45 scientists to develop single particle X-ray diffraction with Free-Electron lasers*

26. Spence JCH, Doak RB: **Single Molecule Diffraction**. *Physical Review Letters* 2004, **92**:198102.
27. Spence JCH, Schmidt K, Wu JS, Hembree G, Weierstall U, Doak B, Fromme P: **Diffraction and imaging from a beam of laser-aligned proteins: resolution limits**. *Acta Crystallographica Section A* 2005, **61**:237-245.
28. Kupper J, Stern S, Holmegaard L, Filsinger F, Rouzee A, Rudenko A, Johnsson P, Martin AV, Adolph M, Aquila A, et al.: **X-Ray Diffraction from Isolated and Strongly Aligned Gas-Phase Molecules with a Free-Electron Laser**. *Physical Review Letters* 2014, **112**.

29. Stroud RM, Agard DA: **Structure determination of asymmetric membrane profiles using an iterative Fourier method**. *Biophys J* 1979, **25**:495-512.
30. Makowski L: **The use of continuous diffraction data as a phase constraint. I. One-dimensional theory**. *J Appl Cryst* 1981, **14**:160–168.
31. Bates R: **Fourier phase problems are uniquely solvable in more than one dimension: 1. Underlying theory**. *Optik* 1982, **61**:247-262.
32. Spence JC, Weierstall U, Fricke TT, Glaeser RM, Downing KH: **Three-dimensional diffractive imaging for crystalline monolayers with one-dimensional compact support**. *J Struct Biol* 2003, **144**:209-218.
33. Spence JCH, Kirian RA, Wang X, Weierstall U, Schmidt KE, White T, Barty A, Chapman HN, Marchesini S, Holton J: **Phasing of coherent femtosecond X-ray diffraction from size-varying nanocrystals**. *Opt. Express* 2011, **19**:2866--2873.
* 34. Kirian RA, Bean RJ, Beyerlein KR, Barthelmess M, Yoon CH, Wang FL, Capotondi F, Pedersoli E, Barty A, Chapman HN: **Direct Phasing of Finite Crystals Illuminated with a Free-Electron Laser**. *Physical Review X* 2015, **5**.
** A proof-of-principle experiment showing that it is possible to directly phase nanocrystal diffraction based on additional information between Bragg peaks. The study was carried out on artificial crystal structures, but showed promise for protein crystals.*
35. Chen JPJ, Millane RP: **Diffraction by nanocrystals**. *J. Opt. Soc. Am. A* 2013, **30**:2627--2634.
36. Kirian RA, Bean RJ, Beyerlein KR, Yefanov OM, White TA, Barty A, Chapman HN: **Phasing coherently illuminated nanocrystals bounded by partial unit cells**. *Philosophical Transactions of the Royal Society B: Biological Sciences* 2014, **369**:20130331.
37. Oszlányi G, Süto A: **The charge flipping algorithm**. *Acta Crystallographica Section A* 2008, **64**:123--134.
* 38. He H, Su W-P: **Direct phasing of protein crystals with high solvent content**. *Acta Crystallographica Section A* 2015, **71**:92--98.
** It had long been argued that crystals with high solvent content could be phased directly using iterative phasing techniques. This was the first to demonstrate it.*
* 39. Millane RP, Arnal RD: **Uniqueness of the macromolecular crystallographic phase problem**. *Acta Crystallographica Section A* 2015, **71**:592--598.
** The full understanding of the information content of Bragg intensities from a crystal are discussed giving conditions under which it should be possible to directly phase these data.*
40. Cowley JM: *Diffraction Physics*: North-Holland; 1981.
41. Doucet J, Benoit JP: **Molecular dynamics studied by analysis of the X-ray diffuse scattering from lysozyme crystals**. *Nature* 1987, **325**:643--646.
42. Wall ME, Ealick SE, Gruner SM: **Three-dimensional diffuse x-ray scattering from crystals of Staphylococcal nuclease**. *Proceedings of the National Academy of Sciences* 1997, **94**:6180-6184.
43. Caspar DLD, Clarage J, Salunke DM, Clarage M: **Liquid-like movements in crystalline insulin**. *Nature* 1988, **332**:659--662.

44. Faure P, Micu A, Perahia D, Doucet J, Smith JC, Benoit JP: **Correlated intramolecular motions and diffuse X-ray scatteringi n lysozyme**. *Nature Struct. Mol. Biol.* 1994, **1**:124--128.
45. Clarage J, Phillips GJ: **Analysis of diffuse scattering and relation to molecular motion**. *Meth. Enzym.* 1997, **277**:407-432.
46. Perez J, Faure P, Benoit JP: **Molecular Rigid-Body Displacements in a Tetragonal Lysozyme Crystal Confirmed by X-ray Diffuse Scattering**. *Acta Crystallographica Section D* 1996, **52**:722--729.
* 47. Van Benschoten AH, Liu L, Gonzalez A, Brewster AS, Sauter NK, Fraser JS, Wall ME: **Measuring and modeling diffuse scattering in protein X-ray crystallography**. *Proceedings of the National Academy of Sciences* 2016, **113**:4069-4074.
** Careful measurements of the continuous diffraction of imperfect macromolecular crystals are carried out to try and gain an understanding of its origin.*
** 48. Ayyer K, Yefanov OM, Oberthür D, Roy-Chowdhury S, Galli L, Mariani V, Basu S, Coe J, Conrad CE, Fromme R, et al.: **Macromolecular diffractive imaging using imperfect crystals**. *Nature* 2016, **530**:202--206.
*** The continuous diffraction of crystals of Photosystem II complexes was found to originate from translational disorder in the crystals. This was directly phased using an iterative algorithm to obtain an electron density image at 3.5 Å resolution.*
49. Chapman H, Yefanov O, Ayyer K, White T, Barty A, Morgan A, Mariani V, Oberthuer D, Pande K, Cryst. JA: **Continuous Diffraction of Molecules and Disordered Molecular Crystals,**. *J. Appl. Cryst* 2017, **in press**.
50. Elser V: **Solution of the crystallographic phase problem by iterated projections**. *Acta Crystallographica A* 2003, **59**:201-209.
51. Meisburger SP, Thomas WC, Watkins MB, Ando N: **X-ray Scattering Studies of Protein Structural Dynamics**. *Chem Rev* 2017, **117**:7615-7672.
52. Wall ME, Adams PD, Fraser JS, Sauter NK: **Diffuse X-Ray Scattering to Model Protein Motions**. *Structure* 2014, **22**:182-184.
53. Yefanov O, Gati C, Bourenkov G, Kirian RA, White TA, Spence JCH, Chapman HN, Barty A: **Mapping the continuous reciprocal space intensity distribution of X-ray serial crystallography**. *Philosophical Transactions of the Royal Society B: Biological Sciences* 2014, **369**.
* 54. Stevenson HP, Lin G, Barnes CO, Sutkeviciute I, Krzysiak T, Weiss SC, Reynolds S, Wu Y, Nagarajan V, Makhov AM, et al.: **Transmission electron microscopy for the evaluation and optimization of crystal growth**. *Acta Crystallogr D Struct Biol* 2016, **72**:603-615.
** This paper describes how cryo-EM can be used to unravel order and defects in 3D nanocrystals*
55. Fromme P, Bottin H, Krauss N, Setif P: **Crystallization and electron paramagnetic resonance characterization of the complex of Photosystem I with its natural electron acceptor ferredoxin**. *Biophysical Journal* 2002, **83**:1760-1773.

(a)

(b)

(c)

real space

reciprocal space

(a)

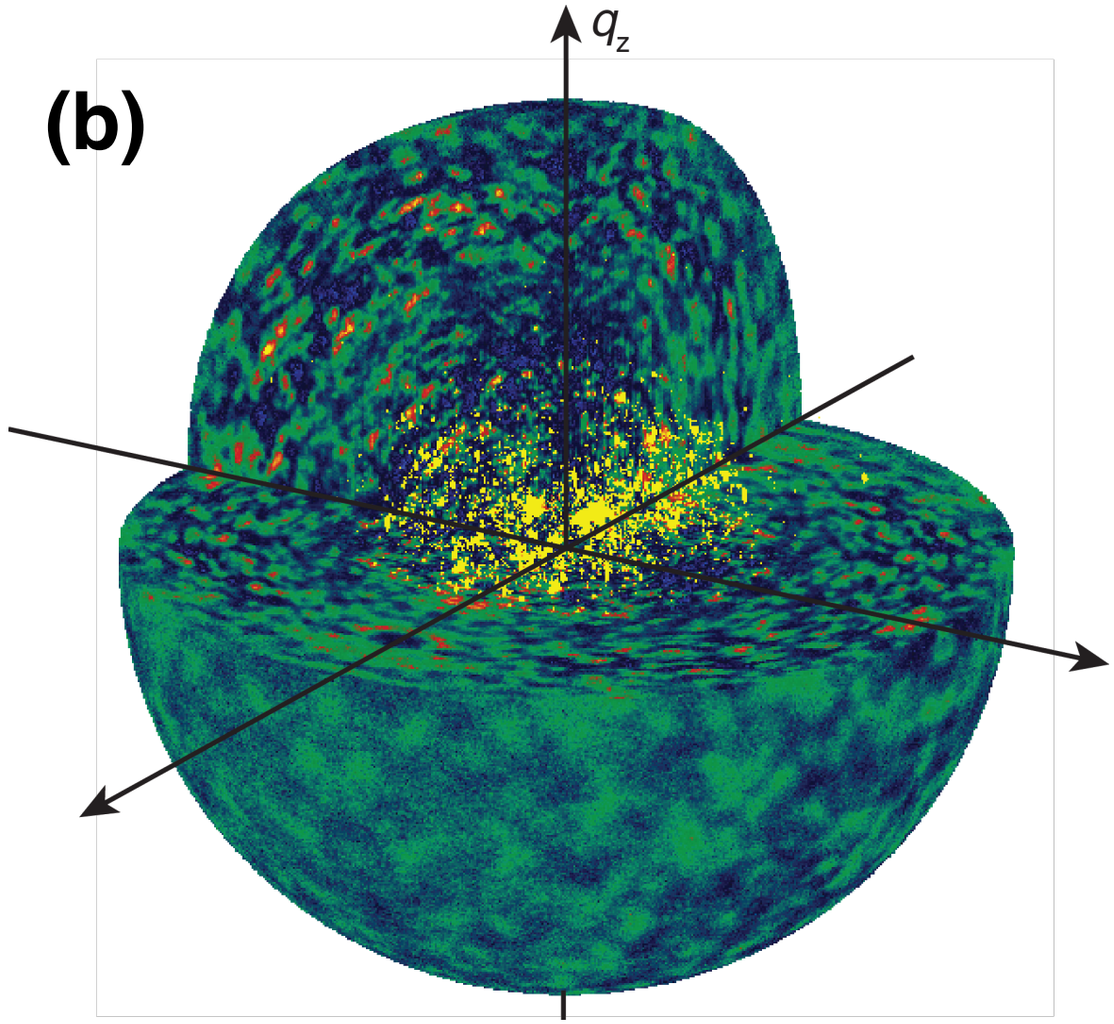

(c)

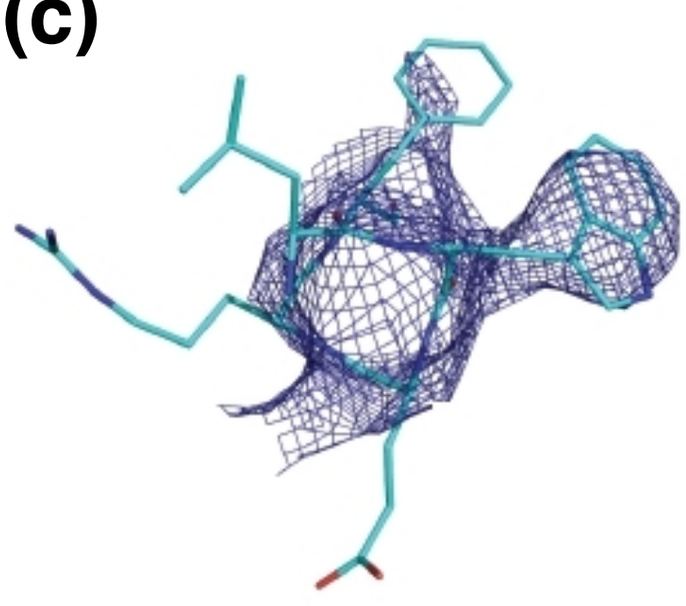

(d)

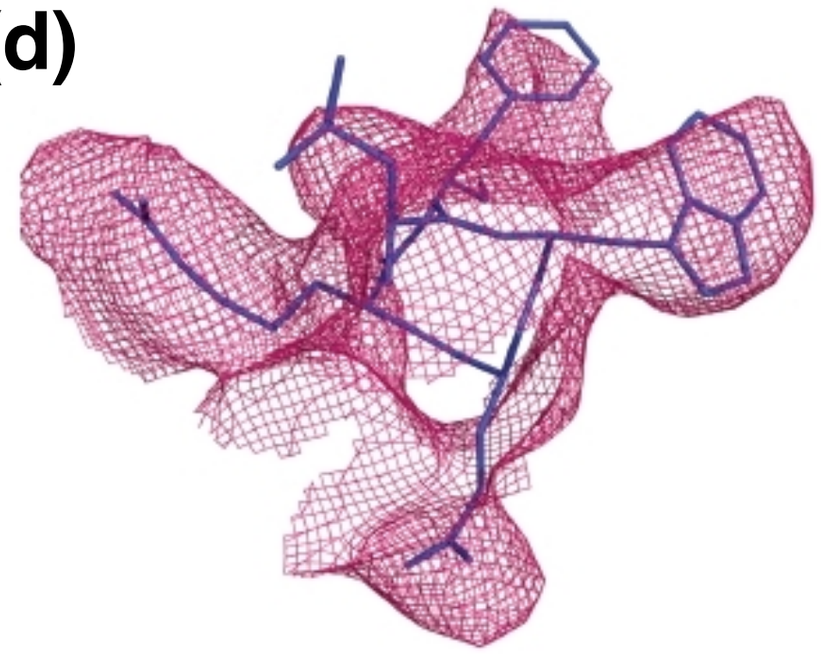

(a)

(b)

(c)

(d)